Since January 2020 Elsevier has created a COVID-19 resource centre with free information in English and Mandarin on the novel coronavirus COVID-19. The COVID-19 resource centre is hosted on Elsevier Connect, the company's public news and information website.

Journal of Hazardous Materials 412 (2021) 125219

Contents lists available at ScienceDirect

Journal of Hazardous Materials

journal homepage: www.elsevier.com/locate/jhazmat

Research paper

High air flow-rate electrostatic sampler for the rapid monitoring of airborne coronavirus and influenza viruses

Hyeong Rae Kim, Sanggwon An, Jungho Hwang *

School of Mechanical Engineering, Yonsei University, Seoul 03722, Republic of Korea

ARTICLE INFO

Editor: Dr. Danmeng Shuai

Keywords:
Airborne virus
Electrostatic air sampler
Viral recovery
Enrichment capacity
Rapid monitoring

ABSTRACT

Capturing virus aerosols in a small volume of liquid is essential when monitoring airborne viruses. As such, aerosol-to-hydrosol enrichment is required to produce a detectable viral sample for real-time quantitative reverse transcription polymerase chain reaction (qRT-PCR) assays. To meet this requirement, the efficient and non-destructive collection of airborne virus particles is needed, while the incoming air flow rate should be sufficiently high to quickly collect a large number of virus particles. To achieve this, we introduced a high air flow-rate electrostatic sampler (HAFES) that collected virus aerosols (human coronavirus 229E, influenza A virus subtypes H1N1 and H3N2, and bacteriophage MS2) in a continuously flowing liquid. Viral collection efficiency was evaluated using aerosol particle counts, while viral recovery rates were assessed using real-time qRT-PCR and plaque assays. An air sampling period of 20 min was sufficient to produce a sample suitable for use in real-time qRT-PCR in a viral epidemic scenario.

1. Introduction

Historically, zoonoses derived from livestock and animals have been the cause of a significant loss of human life and generated severe social costs, though the development of biomedical technology, including the production of antibody drugs and vaccines, has reduced the impact of these infectious diseases to some extent. However, the Middle East respiratory syndrome coronavirus (MERS-CoV), severe acute respiratory syndrome coronavirus (SARS-CoV), influenza A virus (H1N1), and the novel coronavirus appeared in 2019 (SARS-CoV2) are a collection of strongly infectious viruses that continue to mutate. Centers for Disease Control and Prevention (CDC) estimates that there have been 9.2–35.6 million cases of influenza, 140,000–710,000 hospitalizations, and 12,000–56,000 deaths annually since 2010 (CDC, 2020).

The monitoring of biological particles suspended in the air has been used for decades to prevent large-scale outbreaks of infection. Real-time quantitative reverse transcription polymerase chain reaction (qRT-PCR), an assay designed for microbes that works by amplifying a target gene, is the most widely used method for monitoring airborne viruses due to its reliability. Before the assay can be conducted, however, virus aerosols need to be captured in a liquid because liquid samples are required for most bioanalytical approaches (e.g., nucleic acid detection, immunoassays, and cell culturing).

For the rapid monitoring of airborne viruses, it is essential to develop an air sampler that can collect airborne viruses dispersed in the air at very low concentrations and transfer them into a small volume of liquid above the limit of detection (LOD) for real-time qRT-PCR. The enrichment capacity (EC) of aerosol-to-hydrosol (ATH) sampling is an indicator of how many airborne virus particles can be amassed in this small volume of liquid. Thus, a high EC can reduce the time required to produce a detectable virus sample for use in real-time qRT-PCR. In Eq. (1), EC_{ATH} denotes the EC of ATH sampling (Kim et al., 2020a, 2020b):

$$EC_{ATH} = \frac{Q_A \times \eta_{collection}}{Q_L} \quad (1)$$

where Q_A is the flow rate of the air, Q_L is the flow rate of the carrier liquid, and $\eta_{collection}$ is the viral collection efficiency of the air sampler. Yang et al. (2011) reported that there are relatively low concentrations of virus particles in indoor air (10^3–10^4 viral genome copies per 1 m^3 of air) even during an influenza epidemic. Even during the COVID-19 pandemic, low concentrations of the virus (10^3–10^4 viral genome copies per 1 m^3 of air) were detected in a negative-pressure room housing a confirmed patient in an isolation facility (Chia et al., 2020; Santarpia et al., 2020). The LOD of commercial real-time qRT-PCR devices is typically 10^3 viral genome copies per 1 mL of liquid (Drosten et al., 2002; Corman et al., 2020). Based on this, an EC_{ATH} of 10^5 to

* Corresponding author.
E-mail addresses: khr1410@yonsei.ac.kr (H.R. Kim), dkstkdrnjs92@naver.com (S. An), hwangjh@yonsei.ac.kr (J. Hwang).

https://doi.org/10.1016/j.jhazmat.2021.125219
Received 24 September 2020; Received in revised form 2 January 2021; Accepted 21 January 2021
Available online 23 January 2021

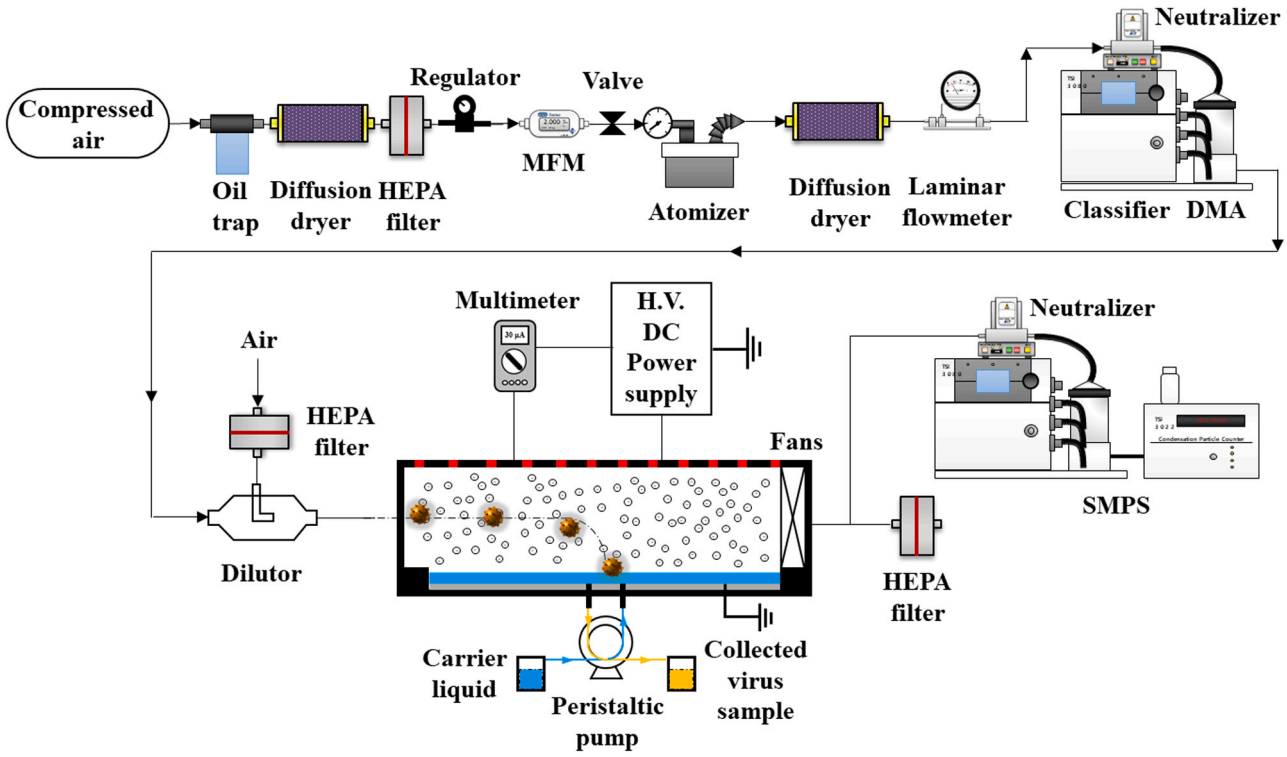

Fig. 1. Experimental setup for the evaluation of airborne virus collection performance of a high air flow-rate electrostatic air sampler (HAFES).

10^6-fold (i.e., from 10^3–10^4 viral genome copies per 1 m^3 of air in a viral epidemic scenario to 10^3 viral genome copies per 1 mL of liquid) is required.

During the air sampling process, airborne virus particles can be damaged by mechanical or chemical stress, rendering them undetectable and leading to a longer sampling time in order to produce a detectable sample, which hinders the rapid monitoring of airborne viruses (Piri et al., 2020; Kim et al., 2018). Therefore, the sampling of airborne virus particles for biosensors and bioassays, including real-time qRT-PCR, needs to be non-destructive, which can be quantified using the recovery rate (R):

$$R = \frac{C_{Recovered}}{C_{ATHsampled}} \tag{2}$$

where $C_{ATH\ sampled}$ is the total concentration of virus particles collected via air sampling, and $C_{Recovered}$ is the concentration of virus particles that are not damaged during the air sampling process.

The SKC BioSampler (SKC Inc., USA) is a widely used ATH sampler that captures airborne biological particles in a liquid (20 mL) using mechanical impaction. However, it has been experimentally proven that the collection efficiency of the SKC BioSampler for nano-sized viruses is less than 50% at a relatively low air sampling flow rate of 12.5 L/min (Li et al., 2018). For example, the EC_{ATH} of the SKC BioSampler for a 20-min sampling period is 6,250. Furthermore, Hong et al. (2016) reported that the SKC BioSampler has low virus recovery rate (1% for T3 bacteriophages) which is a result of the desiccation and degradation of the collected virus particles due to the evaporation of the collection media (Cao et al., 2011). Hong et al. (2016) thus introduced a batch-type electrostatic particle concentrator (EPC) that collects aerosolized virus particles in 0.5 mL of liquid. The collection efficiency of the EPC was found to be 35% with an applied voltage of −10 kV and an air sampling flow rate of 12.5 L/min for 100-nm virus particles. The EC_{ATH} of the EPC with a 20-min sampling period was 96,250, much higher than that of the SKC BioSampler. However, the recovery rate of the collected virus particles remained low (10% for the T3 bacteriophage). Hong et al. believed that the high-intensity electric field employed during the sampling process damaged the collected virus particles (Hong et al., 2016). Amin et al. also reported that long-term exposure to the ozone or reactive oxygen species (ROS) generated by corona discharge during the electrostatic sampling process could damage collected microorganisms (Piri et al., 2020).

Therefore, the air flow rate, viral collection efficiency, and recovery rate of the collected viruses need to be high. This study proposes a high air flow-rate electrostatic air sampler (HAFES) than can achieve an EC_{ATH} higher than 10^5. This study also investigates the use of a continuously flowing carrier liquid because it is essential that the virus sample collected in the liquid is evacuated immediately to prevent exposure to ROS and ozone and thus ensure a high recovery rate. Human coronavirus 229E (HCoV-229E), influenza A virus subtype H1N1 (A/H1N1), influenza A virus subtype H3N2 (A/H3N2), and the MS2 bacteriophage were used as the test viruses. Before the emergence of SARS-CoV, MERS-CoV, and SARS-CoV-2, HCoV-229E was one of the few known coronaviruses to infect humans. A/H1N1, which first appeared in Spain in 1918 and caused between 50 and 100 million deaths, has continued to mutate and causes tens of thousands of deaths in the USA annually (CDC, 2020; Taubenberger et al., 2005). A/H3N2, which caused the Hong Kong flu in 1968, resulting in more than 1 million deaths, mutates into a new form each year and causes the flu (Russell et al., 2008). The MS2 bacteriophage has been widely used to evaluate air sampler performance because its morphology is similar to that of pathogenic viruses, including foot-and-mouth disease (FMD) virus, rhinovirus, and poliovirus (Hong et al., 2016; Verreault et al., 2008; Pan et al., 2016). The HAFES was designed to have a high collection efficiency and recovery rate with a high air flow rate (100 L/min). To achieve this, lab-scale tests were carried out to evaluate the collection efficiency of the HAFES for the test viruses using aerosol counts. The recovery rates of the viruses collected using the HAFES were compared with those collected using the SKC BioSampler with real-time qRT-PCR and plaque assays. Finally, the virus collection performance of the HAFES and the SKC BioSampler was compared using real-time qRT-PCR assays in a simulated viral epidemic scenario.

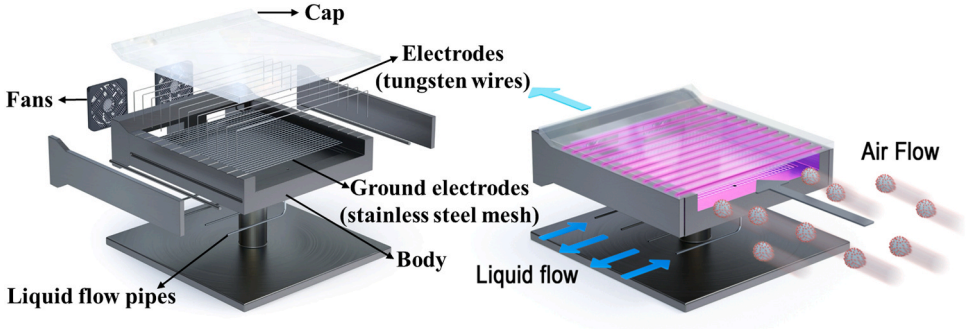

Fig. 2. 3D schematic of the proposed high air flow-rate electrostatic sampler (HAFES).

2. Materials and methods

2.1. Generation and sampling of test viruses

Fig. 1 presents the experimental setup for the virus collection tests using the HAFES. In this study, HCoV-229E (Korea Bank for Pathogenic Viruses, Korea), A/H1N1, A/H3N2 (H-GUARD, Korea), and the MS2 bacteriophage (KORAM Lab-Tech, Korea) were used as test aerosols. Sodium chloride (NaCl; S7653, Sigma-Aldrich, USA) was also used as an aerosol to test the efficiency of size-dependent particle collection. NaCl has been used as a standard material for evaluating particle collection performance of an electrostatic air sampler (Miller et al., 2010; Han et al., 2009; Mainelis et al., 2002). The prepared virus stocks were mixed with deionized water (total volume of 50 mL), and the mixture was atomized using a Collison-type atomizer (9302, TSI Inc., USA). The flow rate of clean compressed air through the atomizer was 2 L/min. A diffusion dryer was used to eliminate moisture from the aerosolized virus particles. The particles passed through a neutralizer (Soft X-ray Charger 4530, HTC, Korea) to generate a Boltzmann charge distribution. The neutralized virus particles entered a differential mobility analyzer (DMA, 3081, TSI Inc., USA). The various-sized virus particles entering the DMA were sorted by size with a classifier (3080, TSI Inc., USA). Using the panel mode (a mode for selectively generating particles of desired size) of the classifier, virus particles of desired size were selectively generated. The selectively generated virus particle sizes were 28, 95, 95, and 109 nm, respectively, for MS2 phage, A/H1N1, A/H3N2, and HCoV-229E. These were similar to those of TEM images (see Section 3.1). The selectively generated virus particles entered the HAFES after 2 L/min of particle-laden air flow had been diluted with clean air. The total air flow rate (40–100 L/min) entering the HAFES was controlled by two fans. In the Section 3 of Supplementary Information, a method for generating the NaCl particles is described in detail.

A 3D model of the proposed HAFES is presented in Fig. 2. The HAFES contained a cap with 12 tungsten-wire electrodes and a body with an air flow inlet and an outlet. The aerosolized virus and NaCl particles entering the HAFES were charged by ions generated on the surface of the discharge electrodes (the tungsten wires) via corona discharge. The charged particles were collected on the ground electrode (stainless-steel mesh) covered by phosphate-buffered saline (PBS, PR2004-100-72, Biosesang, Korea). PBS was continuously supplied through two inlet pipes and the collected virus sample was simultaneously flushed out through two outlet pipes using a peristaltic pump (ISM4408, Ismatec, Germany) with a flow rate of 200 μL/min (Fig. 1).

Corona currents were measured under various air flow rates and applied voltages using a multimeter (8845a, Fluke, USA). I–V measurements were repeated three times. The electrostatic module of COMSOL Multiphysics (Version 5.4) was employed to simulate the electrical potential in the HAFES.

The collection efficiency of the HAFES (Eq. 1) was calculated using Eq. (3):

$$\eta_{collection} = 1 - \frac{C_{on}}{C_{off}} \tag{3}$$

where C_{on} and C_{off} are the concentrations of airborne particles measured at a location downstream the HAFES when the power for corona discharge is on and off, respectively. The size and concentration of the aerosolized virus and NaCl particles were measured using a scanning mobility particle sizer (SMPS, TSI, USA). The SMPS consisted of a classifier (3080, TSI Inc., USA), a DMA (3081, TSI Inc., USA), an aerosol charge neutralizer (Soft X-ray Charger 4530, HCT, Republic of Korea), and a condensation particle counter (CPC, 3775, TSI Inc., USA). The aerosol particles entering the CPC were condensed with butanol to spur growth; these particles then passed through a laser, and the number of particles was counted.

To calculate R (Eq. 2), $C_{ATH\ sampled}$ was defined as follows:

$$C_{ATHsampled} = C_{Entered} \times \eta_{Collection} \tag{4}$$

where $C_{Entered}$ is the total concentration of virus particles entering the air sampler. An SKC button sampler (225–360, SKC Inc., USA) with a liquid-soluble gelatin filter (225–9551, SKC Inc., USA) was used to measure $C_{Entered}$. Aerosolized virus particles were collected on the gelatin filter for 1 min. The collection efficiency of the gelatin filter (225-9551, SKC Inc., USA) is known as almost 100% for airborne viruses (Burton et al., 2007). The virus particle-laden filter was dissolved in 20 mL of PBS for real-time qRT-PCR (HCoV-229E, A/H1N1 and A/H3N2) and plaque assays (the MS2 bacteriophage). To measure $C_{Recovered}$ in Eq. (2), the aerosolized virus particles were collected via the air sampler for 1 min, and the collected virus particles were then diluted with 20 mL of PBS. Li et al. (2018) reported that the collection efficiencies of SKC BioSampler were 40%, 50%, 50%, and 65%, respectively, for particle sizes of 28 nm (MS2 phage), 95 nm (A/H1N1), 95 nm (A/H3N2), and 109 nm (HCoV-229E). Real-time RT-PCR assays were used to determine the $C_{Entered}$ and $C_{Recovered}$ of HCoV-229E, A/H1N1, and A/H3N2 while plaque assays were used to determine the $C_{Entered}$ and $C_{Recovered}$ of the MS2 bacteriophage. Details of the protocol for the real-time qRT-PCR assays are presented in Section 1 of Supplementary Information.

The size of the collected virus particles was measured with a transmission electron microscope (TEM, JEM-1011, JEOL, Japan) and compared with that of the aerosolized virus particles. A collection sample (4 μL) was placed on a TEM grid (3420C-CF, SPI Supplies, USA). After 30 s, materials other than the virus particles were wicked away using filter paper (01531055, ADVANTEC, USA). After this, 4 μL of 1% uranyl acetate (E22400-1, Science Services, Germany) was placed on the grid for 15 s, and filter paper was used to remove the reagent. Another 4 μL of ultra-pure water was used to wash away the residue. The negatively stained virus on the grid was observed after drying for 30 min at room temperature.

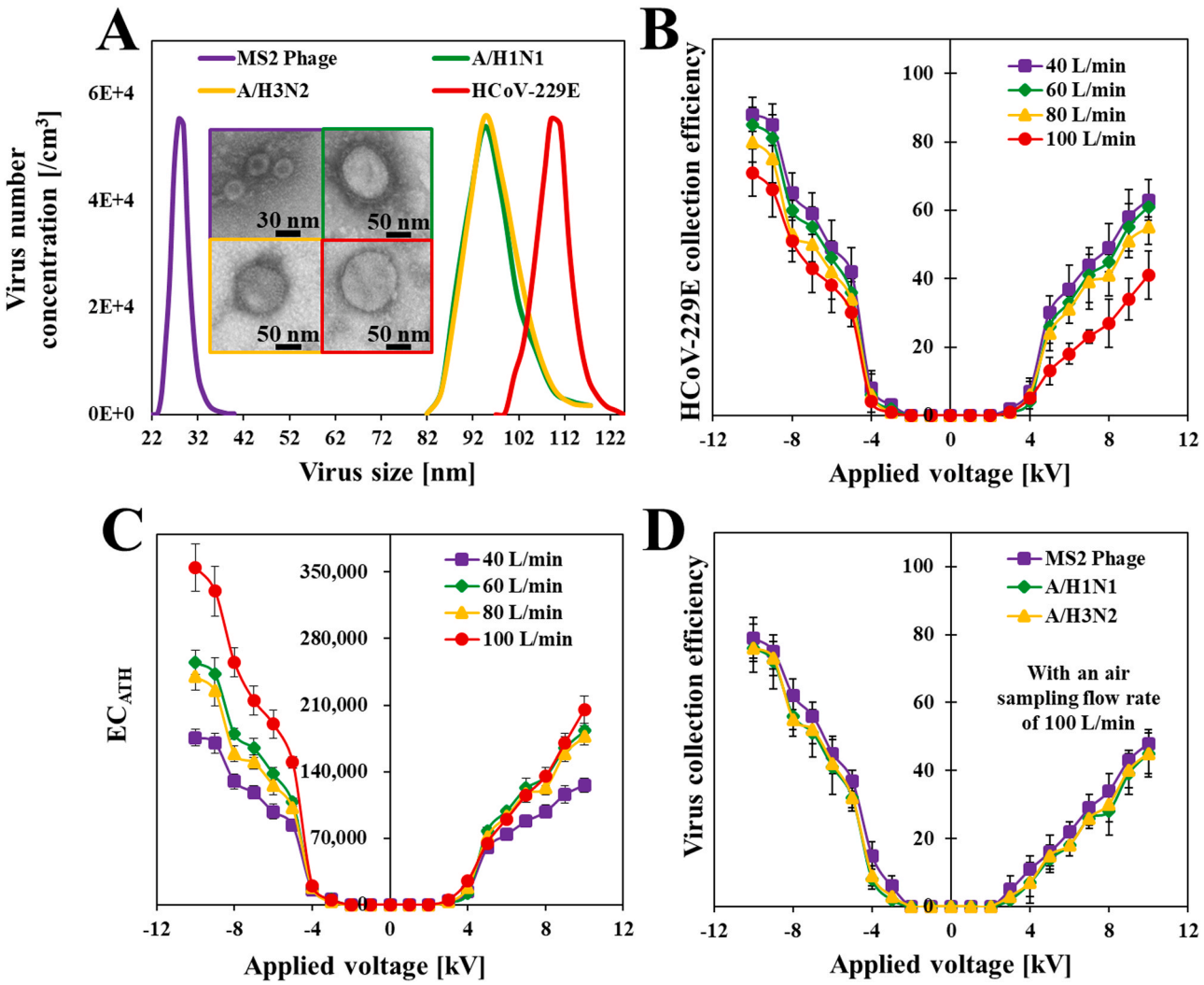

Fig. 3. Characteristics of the aerosolized collection of virus particles using a high air flow-rate electrostatic sampler (HAFES). (A) Size distribution of the aerosolized virus particles and TEM images of virus particles collected using the HAFES. (B) Collection efficiency of the HAFES for human coronavirus 229E (HCoV-229E) under various air flow rates and applied voltages. (C) Aerosol-to-hydrosol enrichment capacity (EC_{ATH}) for HCoV-229E. (D) Collection efficiency for the MS2 bacteriophage, A/H1N1, and A/H3N2 under various applied voltages for an air flow rate of 100 L/min.

2.2. ATH sample preparation in a viral epidemic scenario

The virus sampling performance of the HAFES was compared with that of the SKC BioSampler for A/H1N1 and HCoV-229E, which were aerosolized and collected using the air samplers. According to Yang et al. (2011), the airborne virus concentration in indoor environments (a day-care center, health center, and airplane) during an IAV outbreak varies from 5.8×10^3 to 3.7×10^4 RNA genome copies/m^3. Therefore, for A/H1N1 and HCoV-229E, a concentration of 3.57×10^4 RNA copies/m^3 in the air was used in this study. The virus stocks were diluted with 50 mL of deionized water. The virus solution was then aerosolized using an atomizer with a 2 L/min flow of clean air. After passing through a diffusion dryer and a neutralizer, the airborne virus particles entered the HAFES and the SKC BioSampler. The HAFES was operated with an air flow rate of 100 L/min and an applied voltage of −10 kV. The air flow rate of the SKC BioSampler was 12.5 L/min. The virus particles collected via air sampling were employed in the real-time qRT-PCR analysis. Details of the protocol for real-time qRT-PCR assays are provided in Section 1 of Supplementary Information. The sampling time varied from 20 to 240 min

It was found that 99.0% and 99.7% of the RNA of A/H1N1 and HCoV-229E, respectively, were damaged during aerosolization with the atomizer. Therefore, a concentration of 3.57×10^6 RNA copies/m^3 (100-fold higher than 3.57×10^4 RNA copies/m^3) for A/H1N1 and 1.19×10^7 RNA copies/m^3 (333-fold higher than 3.57×10^4 RNA copies/m^3) for HCoV-229E were aerosolized with the atomizer. The measurement of the concentration (RNA copies/m^3) of the aerosolized virus particles is described in detail in Section 2 of Supplementary Information.

3. Results and discussion

3.1. Virus collection efficiency

Fig. 3(A) presents SMPS data (measured right after the first DMA before entering the dilutor) for the airborne MS2, A/H1N1, A/H3N2, and HCoV-229E, which had peak diameters of 28, 95, 95, and 109 nm, respectively. The inset of Fig. 3(A) shows TEM images of the MS2, A/H1N1, A/H3N2, and HCoV-229E particles collected using the HAFES. The sizes of the collected virus particles were 29, 102, 100, and 115 nm, respectively, similar to the peak diameters and the sizes reported by previous studies (Taubenberger et al., 2005; Russell et al., 2008; Zhu et al., 2020; Merryman et al., 2019).

Fig. 3(B) presents the collection efficiency for aerosolized HCoV-

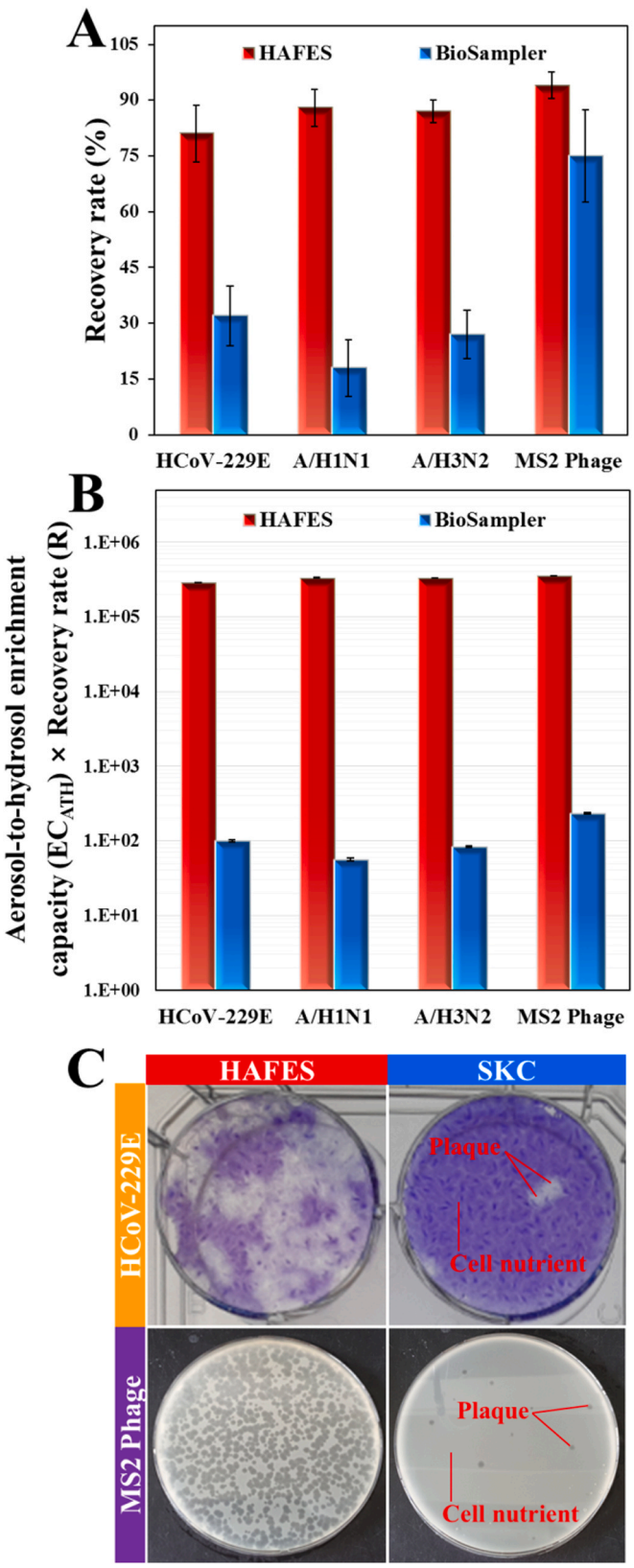

Fig. 4. Comparison between the HAFES and the SKC BioSampler for non-destructive, high-speed virus collection. (A) Recovery rate (R) of the collected virus particles using the HAFES and the SKC BioSampler. (B) Aerosol-to-hydrosol enrichment capacity (EC_{ATH}) × R of the HAFES and the SKC BioSampler for the collected virus particles. (C) Images of plaque-assayed HCoV-229E and MS2 bacteriophage.

229E under various air flow rates and applied voltages. The collection efficiency increased with the applied voltage for a given air flow rate and decreased with the air flow rate for a given voltage. Before testing with the virus aerosols, preliminary tests were conducted using NaCl. Section 3 of the Supplementary Information summarizes the electrical characteristics and aerosol (i.e., NaCl) size-dependent collection efficiency of the HAFES under various air flow rates and applied voltages. We selected an air flow rate of 100 L/min and an applied voltage of −10 kV (collection efficiency of 71 ± 7% for HCoV-229E) for subsequent virus sampling, even though the collection efficiency was 88 ± 5% with an air flow rate of 40 L/min and the same voltage (see Fig. 3(B)). The reason for this choice can be explained by the results for Fig. 3(C), which displays the EC_{ATH} of the HAFES for HCoV-229E under different air flow rates and applied voltages. The highest EC_{ATH} was 355,000 ± 24,850 under the applied voltage of −10 kV and air flow rate of 100 L/min. Therefore, we chose these air flow and voltage settings for subsequent virus sampling.

Fig. 3(D) presents the collection efficiency ($\eta_{collection}$) of the HAFES for the MS2 bacteriophage, A/H1N1, and A/H3N2 under these sampling settings. There were no differences in the collection efficiency for these virus species, even though the MS2 bacteriophage is smaller than that of A/H1N1 and A/H3N2. According to Kim et al. (2020a, 2020b), the collection efficiency of an air sampler such as the HAFES is determined by the combined effects of ionic wind and the Coulombic force. They reported that the collection efficiency due to the ionic wind effect for 30-nm particles (similar to the size of the MS2 bacteriophage) is lower than that for 100-nm particles (similar to the sizes of A/H1N1 and A/H3N2). On the other hand, the collection efficiency due to the Coulombic force effect for 30-nm particles is higher than that for 100-nm particles.

3.2. Enrichment capacity and recovery rate

Fig. 4(A) presents the recovery data for HCoV-229E, A/H1N1, A/H3N2, and the MS2 bacteriophage that were collected using the HAFES and the SKC BioSampler. For HCoV-229E, the recovery rate using the HAFES (81%) was 2.7 times higher than that using the SKC BioSampler (32%). For A/H1N1 and A/H3N2, the recovery rates with the HAFES were 4.9 times (88%) and 3.2 times (87%) higher, respectively, than those with the SKC BioSampler (18% and 27%, respectively). For the MS2 bacteriophage, the HAFES produced a 1.25-times higher recovery rate (94%) than did the SKC BioSampler (75%). More detailed results are available in Section 4 of Supplementary Information (Table S1). The higher viral recovery rate for the HAFES could be because the velocity of the airborne particles in the collection medium using electrostatic sampling is about two to four orders of magnitude lower than when using inertial impaction sampling at comparable air flow rates (Kim et al., 2018; Mainelis, 1999), meaning that the HAFES was likely to be less destructive to the virus particles than was the SCK BioSampler. The ozone concentrations were measured using an ozone counter (OZ 2000G, SERES, France). The results were14 ± 3 ppb, 10 ± 2 ppb, and non-detectable at 0 cm, 3 cm, and 5 cm from the outlet of HAFES, respectively.

Fig. 4(A) also shows that the recovery rates were very similar (81–90%) for HCoV-229E, A/H1N1, A/H3N2, and the MS2 bacteriophage when the HAFES was employed. However, the SKC BioSampler exhibited much lower recovery rates for HCoV-229E (32%) and the influenza viruses (18% and 27% for H1N1 and H3N2, respectively) than for the MS2 bacteriophage (75%). It has been reported in a previous study that influenza viruses generally have a lower recovery rate than the MS2 bacteriophage when an inertia impaction air sampling method is used (Ge et al., 2014). When a large virus particle is captured by the collection media, it experiences a strong inertia force resulting in significant mechanical stress. Therefore, it is more likely that the coronavirus and influenza viruses will be damaged than the MS2 bacteriophage when the same air sampling speed is employed.

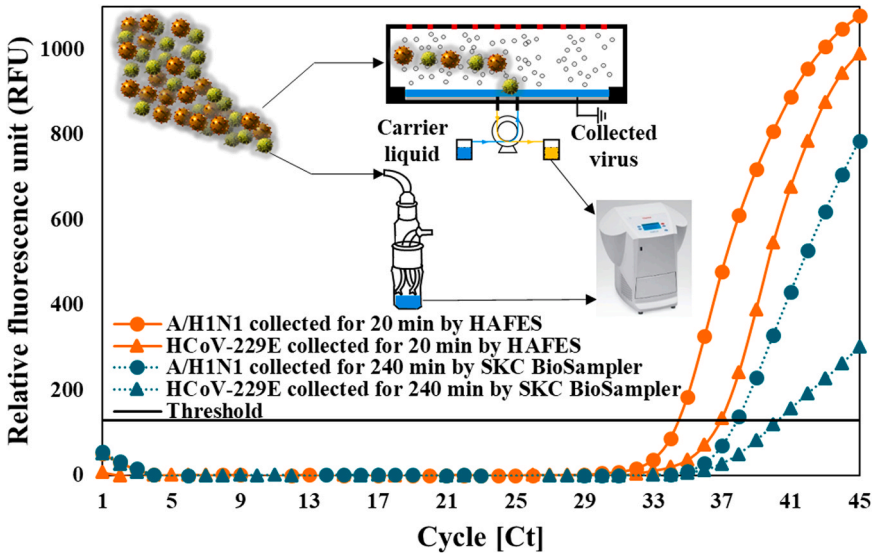

CONFIGURATION	HAFES / HCoV-229E / 20 min	SKC / HCoV-229E / 240 min	HAFES / A/H1N1 / 20 min	SKC / A/H1N1 / 240 min
Concentration [RNA copies/mL]	7,600	1,200	9,600	510
Ct value of real-time qRT-PCR	37.2	39.9	33.8	38.1

Fig. 5. Real-time qRT-PCR assays for virus particles collected using an aerosol-to-hydrosol approach with the HAFES and the BioSampler in a viral epidemic scenario.

The recovery rate for the MS2 bacteriophage collected using the HAFES was compared with the recovery rates obtained using the batch-type EPC and a continuous-type electrostatic ATH sampler (ATHS) (Hong et al., 2016; Park et al., 2016). The recovery rate for the MS2 bacteriophage with the HAFES (94%) was higher than that with the ATHS (59%) and the EPC (55%). Further details are presented in Section 5 of Supplementary Information (Fig. S3(A)).

Fig. 4(B) presents the EC_{ATH} × R values using the HAFES and the SKC BioSampler for HCoV-229E, A/H1N1, A/H3N2, and the MS2 bacteriophage. The SKC BioSampler produced EC_{ATH} × R values of 100.0, 56.3, 83.4, and 234.4 for HCoV-229E, A/H1N1, A/H3N2, and the MS2 bacteriophage, respectively. On the other hand, HAFES achieved EC_{ATH} × R values of 287,550, 334,440, 330,600, and 357,200 for HCoV-229E, A/H1N1, A/H3N2, and the MS2 bacteriophage, respectively. Therefore, viral samples that were 1,524 to 5,945 times more concentrated were obtained using the HAFES. In addition, the EC_{ATH} × R values for the HAFES (357,200) were much higher than those for the ATHS (14,160) and the EPC (4,813) when sampling the MS2 bacteriophage. Section 5 of Supplementary Information (Fig. S3(B)) provides more detailed information.

Fig. 4(C) displays images of cultured viral plates of HCoV-229E and the MS2 bacteriophage collected using the HAFES and the SKC BioSampler. The numbers of viral plaques observed from the HAFES, for HCoV-229E and MS2 bacteriophage, were 10 times and over 100 times higher than those from the SKC Biosampler for HCoV-229E and MS2 bacteriophage, respectively.

3.3. Detectable sample production in a simulated viral epidemic scenario

A/H1N1 and HCoV-229E particles at a concentration of 3.57×10^4 RNA copies/m^3 were separately suspended in the air to simulate a viral epidemic scenario. Fig. 5 presents real-time qRT-PCR amplification curves for the virus samples collected using the HAFES and the SKC BioSampler and the corresponding concentrations and cycle threshold (Ct). The concentrations of the HCoV-229E and A/H1N1 samples collected over 20 min using the HAFES were 7,600 RNA copies/mL (Ct = 37.2) and 9,600 RNA copies/mL (Ct = 33.8), respectively. In contrast, the concentrations of the HCoV-229E and A/H1N1 samples collected using the SKC BioSampler were 1,200 RNA copies/mL (Ct = 39.9) and 510 RNA copies/mL (Ct = 38.1), respectively, for a collection time of 240 min. The HCoV-229E and A/H1N1 samples using the SKC BioSampler for a virus sampling time of under 240 min (i.e., 20, 60, 110, 160, and 200 min) were not detectable and not amplified by real-time qRT-PCR. On the other hand, Fig. 5 confirms that a sampling time of 20 min was sufficient to produce detectable samples for real-time qRT-PCR when using the HAFES in a viral epidemic scenario.

4. Conclusions

The HAFES was able to rapidly capture airborne viruses with a high collection efficiency even at a high air flow rate (71%, 79%, 76%, and 76% for HCoV-229E, the MS2 bacteriophage, A/H1N1, and A/H3N2, respectively, with an air flow rate of 100 L/min and an applied voltage of −10 kV). The HAFES produced high viral recovery rates for all viruses (81%, 94%, 88%, and 87% for HCoV-229E, the MS2 bacteriophage, A/H1N1, and A/H3N2, respectively, with an air flow rate of 100 L/min and an applied voltage of −10 kV). The ATH enrichment capacity (EC_{ATH}) × recovery rate (R) for the HAFES was 287,550, 334,440, 330,600, and 357,200 for HCoV-229E, IAV H1N1, IAV H3N2, and the MS2 bacteriophage, respectively. It was also proven that an airborne viral sampling time of 20 min was sufficient to produce a detectable real-time qRT-PCR sample in a simulated viral epidemic scenario with the HAFES. In conclusion, the HAFES can be utilized in field environments where the concentration of airborne virus particles is low for rapid viral monitoring and efficient air quality management.

CRediT authorship contribution statement

Hyeong Rae Kim: Conceptualization, Investigation, Writing - original draft. **Sanggwon An**: Investigation, Validation. **Jungho Hwang**: Funding acquisition, Writing - review & editing, Supervision.

Declaration of Competing Interest

The authors declare that they have no known competing financial interests or personal relationships that could have appeared to influence the work reported in this paper.

Acknowledgments

This work was supported by the Technology Innovation Program-Industrial Technology Alchemist Project (20012215, Intelligent platform for in-situ virus detection and analysis) funded by the Ministry of Trade, Industry and Energy, Korea (MOTIE, Korea).

Appendix A. Supporting information

Supplementary data associated with this article can be found in the online version at doi:10.1016/j.jhazmat.2021.125219.

References

Burton, N.C., Grinshpun, S.A., Reponen, T., 2007. Physical collection efficiency of filter materials for bacteria and viruses. Ann. Occup. Hyg. 51 (2), 143–151.

Cao, G., Noti, J.D., Blachere, F.M., Lindsley, W.G., Beezhold, D.H., 2011. Development of an improved methodology to detect infectious airborne influenza virus using the NIOSH bioaerosol sampler. J. Environ. Monit. 13, 3321–3328.

CDC, 2020. https://www.cdc.gov/flu/about/disease/burden.htm (Accessed 15 September 2020).

Chia, P.Y., Coleman, K.K., Tan, Y.K., Ong, S.W.X., Gum, M., Lau, S.K., Lim, X.F., Lim, A. S., Sutjipto, S., Lee, P.H., Son, T.T., Young, B.E., Milton, D.K., Gray, G.C., Schuster, S., Barkham, T., De, P.P., Vasoo, S., Chan, M., Ang, B.S.P., Tan, B.H., Leo, Y.-S., Ng, O.-T., Wong, M.S.Y., Marimuthu, K., 2020. Detection of air and surface contamination by SARS-CoV-2 in hospital rooms of infected patients. Nat. Commun. 11 (1), 1–7.

Corman, V.M., Landt, O., Kaiser, M., Molenkamp, R., Meijer, A., Chu, D.K., Bleicker, T., Brünink, S., Schneider, J., Schmidt, M.L., Mulders, D.G., Haagmans, B.L., Veer, B. v d, Brink, S. v d, Wijsman, L., Goderski, G., Romette, J.-L., Ellis, J., Zambon, M., Pelris, M., Goossens, H., Reusken, C., Koopmans, M.P., Drosten, C., 2020. Detection of 2019 novel coronavirus (2019-nCoV) by real-time RT-PCR. Eurosurveillance 25 (3), 2000045.

Drosten, C., Gottig, S., Schilling, S., Asper, M., Panning, M., Schmitz, H., Gunther, S., 2002. Rapid detection and quantification of RNA of Ebola and Marburg viruses, Lassa virus, Crimean-Congo Hemorrhagic Fever virus, Rift Valley Fever virus, Dengue virus, and Yellow Fever virus by real-time reverse transcription-PCR. J. Clin. Microbiol. 20, 2323–2330.

Ge, S., Kuehn, T.H., Abin, M., Verma, H., Becele, A., Mor, S.K., Goyal, S.M., Appert, J., Raynor, P.C., Zuo, Z., 2014. Airborne virus survivability during long-term sampling using a non-viable Andersen cascade impactor in an environmental chamber. Aerosol Sci. Technol. 48, 1360–1368.

Han, B., Hudda, N., Ning, Z., Kim, Y.J., Sioutas, C., 2009. Efficient collection of atmospheric aerosols with a particle concentrator—electrostatic precipitator sampler. Aerosol Sci. Technol. 43 (8), 757–766.

Hong, S., Bhardwaj, J., Han, C.H., Jang, J., 2016. Gentle sampling of submicrometer airborne virus particles using a personal electrostatic particle concentrator. Environ. Sci. Technol. 50, 12365–12372.

Kim, H.R., Park, J.W., Kim, H.S., Yong, D., Hwang, J., 2018. Comparison of lab-made electrostatic rod-type sampler with single stage viable impactor for identification of indoor airborne bacteria. J. Aerosol Sci. 115, 190–197.

Kim, H.R., An, S., Hwang, J., 2020a. Aerosol-to-hydrosol sampling and simultaneous enrichment of airborne bacteria for rapid biosensing. ACS Sens. 5, 2763–2771.

Kim, S., Yu, T.U., Hwang, J., 2020b. Numerical investigation of the separation mechanism in an electrostatic aerosol-to-hydrosol separator by glow corona discharge: a quantitative comparison of the effects of ionic wind and Coulomb force. Plasma Sources Sci. Technol. 29, 075008.

Li, J., Leavey, A., Wang, Y., O'Neil, C., Wallace, M.A., Burnham, C.A.D., Boon, A.C., Babcock, H., Biswas, P., 2018. Comparing the performance of 3 bioaerosol samplers for influenza virus. J. Aerosol Sci. 115, 133–145.

Mainelis, G., 1999. Collection of airborne microorganisms by electrostatic precipitation. Aerosol Sci. Technol. 30, 127–144.

Mainelis, G., Willeke, K., Adhikari, A., Reponen, T., Grinshpun, S.A., 2002. Design and collection efficiency of a new electrostatic precipitator for bioaerosol collection. Aerosol Sci. Technol. 36 (11), 1073–1085.

Merryman, A.E., Sabaraya, I.V., Rowles III, L.S., Toteja, A., Carrillo, S.I., Sabo-Attwood, T., Saleh, N.B., 2019. Interaction between functionalized multiwalled carbon nanotubes and MS2 bacteriophages in water. Sci. Total Environ. 670, 1140–1145.

Miller, A., Frey, G., King, G., Sunderman, C., 2010. A handheld electrostatic precipitator for sampling airborne particles and nanoparticles. Aerosol Sci. Technol. 44 (6), 417–427.

Pan, M., Eiguren-Fernandez, A., Hsieh, H., Afshar-Mohajer, N., Hering, S.V., Lednicky, J., Fan, Z.H., Wu, C.-Y., 2016. Efficient collection of viable virus aerosol through laminar-flow, water-based condensational particle growth. J. Appl. Microbiol. 120, 805–815.

Park, J.W., Kim, H.R., Hwang, J., 2016. Continuous and real-time bioaerosol monitoring by combined aerosol-to-hydrosol sampling and ATP bioluminescence assay. Anal. Chim. Acta 941, 101–107.

Piri, A., Kim, H.R., Hwang, J., 2020. Prevention of damage caused by corona discharge-generated reactive oxygen species under electrostatic aerosol-to-hydrosol sampling. J. Hazard. Mater. 384, 121477.

Russell, C.A., Jones, T.C., Barr, I.G., Cox, N.J., Garten, R.J., Gregory, V., Gust, I.D., Hampson, A.W., Hay, A.J., Hurt, A.C., de Jong, J.C., Kelso, A., Klimov, A.I., Kageyama, T., Komadina, N., Lapedes, A.S., Lin, Y.P., Mosterin, A., Obuchi, M., Odagiri, T., Osterhaus, A.D.M.E., Rimmelzwaan, G.F., Shaw, M.W., Skepner, E., Stohr, K., Tashiro, M., Fouchier, R.A.M., Smith, D.J., 2008. The global circulation of seasonal influenza A (H3N2) viruses. Science 320, 340–346.

Santarpia, J.L., Rivera, D.N., Herrera, V., Morwitzer, M.J., Creager, H., Santarpia, G.W., Crown, K.K., Brett-Major, D.M., Schnaubelt, E.R., Broadhurst, M.J., Lawler, J.V., Reid, S.P., Lowe, J.J., 2020. Aerosol and surface transmission potential of SARS-CoV-2. medRxiv.

Taubenberger, J.K., Reid, A.H., Lourens, R.M., Wang, R., Jin, G., Fanning, T.G., 2005. Characterization of the 1918 influenza virus polymerase genes. Nature 437, 889–893.

Verreault, D., Moineau, S., Duchaine, C., 2008. Methods for sampling of airborne viruses. Microbiol. Mol. Biol. Rev. 72, 413–444.

Yang, W., Elankumaran, S., Marr, L.C., 2011. Concentrations and size distributions of airborne influenza A viruses measured indoors at a health centre, a day-care centre and on aeroplanes. J. R. Soc. Interface 8, 1176–1184.

Zhu, N., Zhang, D., Wang, W., Li, X., Yang, B., Song, J., Zhao, X., Huang, B., Shi, W., Lu, R., Niu, P., Zhan, F., Ma, X., Wang, D., Xu, W., Wu, G., Gao, G.F., Phil, D., Tan, W., 2020. A novel coronavirus from patients with pneumonia in China, 2019. N. Engl. J. Med. 382, 727–733.